Analysis of Frequency Offset Effect on PRACH in 5G NR Systems

Wenxi He(✉), Yifan Du, and Hang Long

Wireless Signal Processing and Network Lab, Key Laboratory of Universal Wireless Communication, Ministry of Education Beijing University of Posts and Telecommunications, Beijing, China
bupthewenxi@163.com

Abstract. Physical Random Access Channel (PRACH) in 5G new radio (NR) systems transmits random access preamble for the user equipment (UE) to access the network. In 5G NR systems, Zadoff-Chu (ZC) sequences are used as random access preamble sequences. Frequency offset severely affects the perfect autocorrelation properties of the preamble sequences, thereby affecting the preamble detection performance and timing accuracy. In this paper, frequency offset effect on PRACH preamble miss detection rate and timing error in 5G NR systems is analyzed. Firstly, the frequency offset effect on inter-carrier interference and the correlation of general sequences is derived. Then, based on the former derivation and characteristics of ZC sequences, the frequency offset effect on correlation of ZC sequences is derived. Moreover, PRACH preamble miss detection rate and timing error are analyzed. The analytical results show that for different random access UEs with different PRACH preamble numbers, the random access performances are differently affected by the same frequency offset. Besides, the higher miss detection rate, the smaller timing error. The simulation results show the rationality of the analysis.

Keywords: PRACH · Frequency offset · Correlation

1 Introduction

The random access procedure is of great importance for the user equipment (UE) to access the network and achieve timing synchronization with the gNodeB (gNB). As an initial step to connect to the network, one UE sends a preamble which carries access information (control and timing information) through Physical Random Access Channel (PRACH) [1], and the gNB needs to detect the preamble to identify the random access preamble number and obtain timing information to calculate timing advance (TA) value [2]. Then the UE can establish a connection with the network and achieve timing synchronization with the

Supported by China Unicom Network Technology Research Institute and project 61302088 which was supported by National Natural Science Foundation of China.

H. Gao et al. (Eds.): ChinaCom 2019, LNICST 312, pp. 679–692, 2020.
https://doi.org/10.1007/978-3-030-41114-5_51

base station [3]. The peak-to-average ratio (PAR) and peak position of correlation are usually used to detect PRACH preamble sequences and obtain timing information. Zadoff-Chu (ZC) sequences are used as random access preamble sequences in 5G new radio (NR) systems due to the good autocorrelation properties and periodic cross-correlation properties [4].

Frequency offset affects the orthogonality between subcarriers, thus affecting the accurate reception of preamble sequences and the correlation result at the receiver. Ultimately, frequency offset will affect the performance of preamble detection and timing accuracy. The high speed railway communication has been incorporated into 5G NR systems as a special scenario, so it is necessary to study frequency offset effect on PRACH and corresponding solutions in 5G NR Systems [5].

For solving the above problem, there are already some studies. Ref. [6] proposes a Peak Ratio based Estimation method to estimate the frequency offset between a mobile phone and the infrastructure based on PRACH preambles. This method use the ratio of the largest peak value over the second largest peak value to estimate frequency offset. However, this method does not take into account that frequency offset has different effect on detection performance of different preamble sequences. Ref. [7] introduces an analytical framework quantifying the ZC sequence's performance, and it demonstrates that the frequency offset immunity of a ZC sequence set can be controlled by shaping the spectrum of the ZC sequence set. But with the advancement of the 3GPP protocol, the type of restricted sets are determined to adapt to the high speed scenes, the above analytical framework is of little significance in 5G NR systems. So analysis of the frequency offset effect on the PRACH preamble sequences in 5G NR systems is needed.

In this paper, based on the analysis of the frequency offset effect on correlation of ZC sequences, the PRACH preamble detection performance and timing accuracy affected by the frequency offset are derived. Considering the average value of correlation does not change much when the signal and noise power are determined, the peak size is used to analyze the preamble detection performance in this paper. The analysis is performed in the frequency domain and based on the preamble transmit and receive processes in 5G NR systems. By analyzing the frequency offset effect on inter-carrier interference, general conclusion about frequency offset effect on the peak of correlation result is derived. Then, combining the characteristics of ZC sequences with the derived general conclusion, frequency offset effect on the PRACH is analyzed. The PRACH preamble detection Block Error Ratio (BLER) and Cumulative Distribution Function (CDF) of TA error are taken as two performance metrics. The analysis show that under the impact of frequency offset, the PRACH preamble detection performance and timing accuracy of different PRACH preamble sequences are different. The higher the PRACH preamble detection BLER, the lower TA error. Through simulation, the rationality of the whole analysis is verified.

The remainder of this paper is organized as follows. Section 2 mainly describes the system model, and Sect. 3 elaborates the analysis and inferences, including

the frequency offset effect on subcarriers and the peak of correlation result. Section 4 deduces the specific effect of frequency offset on the PRACH. Section 5 shows the simulation results and proves the rationality of analysis. Finally Sect. 6 concludes this paper.

Notations: Sequences with uppercase letter Y denotes frequency-domain sequences, with lowercase letter x denotes time-domain sequences.

2 System Model

2.1 Preamble Transmitter

The general process of PRACH Preamble transmitter is shown in Fig. 1. Where $x(m)$ refers to the random-access preamble sequence, and its size is N_{seq}. $Y_1(n)$ refers to its frequency-domain representation and is calculated by DFT as

$$Y_1(n) = \sum_{m=0}^{N_{seq}-1} x(m)\mathrm{e}^{-j\frac{2\pi mn}{N_{seq}}} \quad n = 0,1,\cdots,N_{seq}-1 \tag{1}$$

By mapping $Y_1(n)$ to the middle of N subcarriers, we can get a frequency-domain sequence $Y_2(n)$. $x_s(p)$ refers to the sending signal which is the time-domain representation of $Y_2(n)$, where the IFFT size is N.

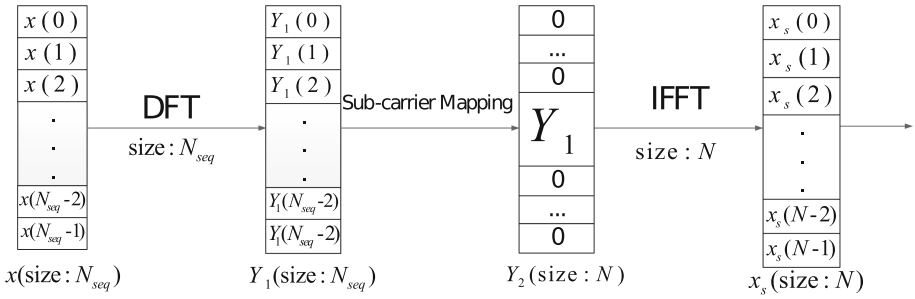

Fig. 1. The general process of PRACH Preamble transmitter.

2.2 Preamble Detector

At the receiver, the received time-domain preamble sequence $x_r(p)$ can be denoted as

$$x_r(p) = Hx_s(p)\mathrm{e}^{j\frac{2\pi\Delta f}{f_s}p} + q(p) \quad p = 0,1,\cdots,N-1 \tag{2}$$

where H is the Line of Sight (LOS) channel gain, Δf refers to the Doppler shift, f_s is bandwidth of one subcarrier, and $q(p)$ refers to the noise [8]. The general process of PRACH Preamble detector is shown in Fig. 2. For the received sequence,

after DFT and subcarrier de-mapping, we can get a frequency-domain sequence $Y_4(n)$. To facilitate calculation and analysis, we implement cross-correlation calculation between the received sequence and the root sequence in the frequency domain. In Fig. 2, $Y_{root}(n)$ refers to the frequency-domain representation of the root sequence $x_{root}(m)$, which is defined in 5G NR specifications. $Y_c(n)$ is calculated as

$$Y_c(n) = Y_4(n) \times Y_{root}(n)^* \tag{3}$$

$x_c(p)$ refers to the time-domain cross-correlation result between the received sequence and the root sequence, and its size is N. By detecting the peak size and peak position of the absolute value of $x_c(p)$, we can determine which UE send the preamble and obtain TA value.

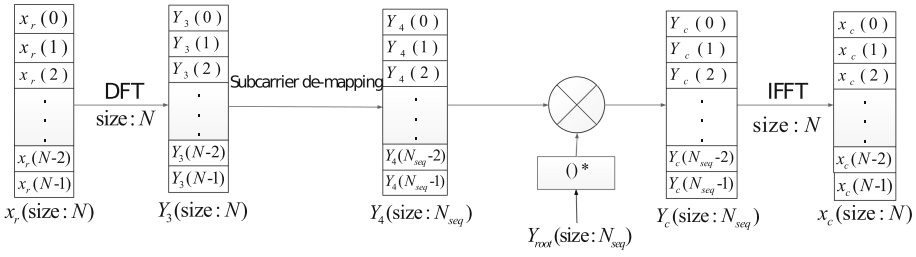

Fig. 2. The general process of PRACH Preamble detector.

3 Frequency Offset Effect on General Sequences

3.1 Frequency Offset Effect on Subcarriers

In this section, it is analyzed how frequency offset affects the orthogonality between subcarriers. Firstly, the specific influence of frequency offset on subcarriers will be analyzed by a simple frequency domain sequence, where the d-th entry is 1, and others are 0. Let

$$Y_2(z) = \begin{cases} 1 & z = d \\ 0 & \text{else} \end{cases} \quad z = 0, 1, \cdots, N-1 \tag{4}$$

According to Fig. 1, $x_s(p)$ can be obtained by IFFT as

$$x_s(p) = \frac{1}{N} \mathrm{e}^{\frac{j2\pi dp}{N}} \tag{5}$$

Only consider frequency offset effect, set $H = 1$ and $q = 0$, according to (2), $x_r(p)$ is obtained as

$$x_r(p) = \frac{1}{N} \mathrm{e}^{\frac{j2\pi(\Delta f + df_s)p}{Nf_s}} \tag{6}$$

After DFT, $Y_3(z)$ is obtained as

$$Y_3(z) = \frac{1}{N} \times \frac{\sin\left(\frac{\Delta f + df_s - zf_s}{f_s}\pi\right)}{\sin\left(\frac{\Delta f + df_s - zf_s}{Nf_s}\pi\right)} e^{j\left(\frac{\Delta f + df_s - zf_s}{f_s} - \frac{\Delta f + df_s - zf_s}{Nf_s}\right)\pi} \tag{7}$$

By comparing $Y_2(z)$ and $Y_3(z)$, it is known that only consider the impact of frequency offset, the received sequence $Y_3(z)$ can be expressed by $Y_2(z)$ as

$$Y_3(z) = \sum_{z_1=0}^{N-1} Y_2(z_1) K(z_1 - z) \tag{8}$$

where $K(z_1 - z)$ refers to the interference coefficient of inter-carrier interference and can be denoted as follows

$$K(l) = \begin{cases} \frac{1}{N} e^{j\theta_0} \left| \frac{\sin(\frac{\Delta f}{f_s}\pi)}{\sin(\frac{\Delta f + lf_s}{Nf_s}\pi)} \right| e^{j(\frac{-l}{N})\pi} & 0 \le l \le N-1 \\ \frac{1}{N} e^{j\theta_0} \left| \frac{\sin(\frac{\Delta f}{f_s}\pi)}{\sin(\frac{\Delta f + lf_s}{Nf_s}\pi)} \right| e^{j(\frac{-l}{N}+1)\pi} & -(N-1) \le l < 0 \end{cases} \tag{9}$$

$$\theta_0 = \frac{(N-1)\Delta f \pi}{Nf_s}$$

where θ_0 is the phase of $K(0)$, From (9), it is easier to get the following conclusions

- There is a sudden change of π between the phase of $K(-1)$ and θ_0.
- Regardless of the phase mutation, the phase difference between two adjacent items is $\frac{\pi}{N}$.
- The absolute value of $K(0)$ is the largest in $K(l)$, and the absolute value of $K(-1)$ is the second largest.
- The larger the absolute value of l, the smaller the absolute value of $K(l)$, so the farther a subcarrier is from the current subcarrier, the smaller the impact of the subcarrier on the current subcarrier.

Combine the above conclusions with (2), the received frequency-domain sequence after de-mapping affected by frequency offset can be denoted as

$$Y_4(n) = He^{j\theta_0} \left[\sum_{k=n}^{N_{seq}-1} Y_1(k) \left|K(k-n)\right| e^{j\frac{(n-k)\pi}{N}} - \sum_{k=0}^{n-1} Y_1(k) \left|K(k-n)\right| e^{j\frac{(n-k)\pi}{N}} \right] + \mathrm{Q}(n) \tag{10}$$

According to (9) and (10), it is easier to get that the closer k is to n, the larger $|K(k-n)|$ is, and the closer $e^{j\frac{(n-k)\pi}{N}}$ is to 1. Considering that the size of IFFT N is often much larger than the size of preamble sequence N_{seq}, and

$|n-k|$ is smaller than N_{seq}. So the impact of $e^{j\frac{(n-k)\pi}{N}}$ can be ignored. Then $Y_4(n)$ can be simplified and approximated as

$$\begin{aligned} Y_4(n) \approx H e^{j\theta_0} &\left[|K(0)|\, Y_1(n) + \sum_{k=1}^{N_{seq}-1} |K(k)|\, Y_{1,k}(n) - \sum_{k=1-N_{seq}}^{-1} |K(k)|\, Y_{1,k}(n) \right] \\ &+ \mathrm{Q}(n) \\ k = -(N_{seq}-1), -(N_{seq}-2), \cdots, -1, 1, 2, \cdots, N_{seq}-2, N_{seq}-1 & \end{aligned} \tag{11}$$

where $Y_{1,k}(n)$ is the k-th entry interference and can be denoted by $Y_1(n)$ as

$$Y_{1,k}(n) = \left\{ \begin{array}{ll} Y_1(n+k) & \max(0,\text{-}k) \le n \le \min(N_{seq}-1, N_{seq}-1-k) \\ 0 & \text{else} \end{array} \right\} \tag{12}$$

So the received frequency-domain sequence affected by frequency offset is simply denoted by the sending sequence.

3.2 Frequency Offset Effect on Correlation

In the previous section, we analysis the frequency offset effect on subcarriers, and derive expression of the received frequency-domain sequence $Y_4(n)$ affected by frequency offset. In this section, it is theoretically analyzed how the peak of correlation result can be affected by the frequency offset. According to (3) and (11), $Y_c(n)$ is obtained as

$$\begin{aligned} Y_c(n) \approx & H e^{j\theta_0} \left[|K(0)| Y_1(n) + \sum_{k=1}^{N_{seq}-1} |K(k)| Y_{1,k}(n) - \sum_{k=1-N_{seq}}^{-1} |K(k)| Y_{1,k}(n) \right] \\ & \times Y_{root}(n)^* + \mathrm{Q}(n) Y_{root}(n)^* \end{aligned} \tag{13}$$

where $e^{j\theta_0}$ has no effect on the absolute value of the cross-correlation result, and can be ignored. To compare the cross-correlation with or without affected by the frequency offset, set

$$\begin{aligned} Y_{c,pre}(n) &= H Y_1(n) Y_{root}(n)^* \\ Y_{c,interf}(n) &= \sum_{k=1}^{N_{seq}-1} Y_{c,interf,k}(n) - \sum_{k=1-N_{seq}}^{-1} Y_{c,interf,k}(n) \\ Y_{c,interf,k}(n) &= H |K(k)| Y_{1,k}(n) Y_{root}(n)^* \end{aligned} \tag{14}$$

Then $Y_c(n)$ and $x_c(p)$ affected by the frequency offset can be denoted as

$$\begin{aligned} Y_c(n) &= |K(0)| Y_{c,pre}(n) + Y_{c,interf}(n) + \mathrm{Q}(n) Y_{root}(n)^* \\ x_c(p) &= |K(0)| x_{c,pre}(p) + x_{c,interf}(p) + q_{cor}(p) \end{aligned} \tag{15}$$

where $x_{c,pre}(p)$, $x_{c,interf}(p)$, $q_{cor}(p)$ are the time-domain representation of $Y_{c,pre}(n)$, $Y_{c,interf}(n)$, $\mathrm{Q}(n)Y_{root}(n)^*$, respectively. Set the time-domain representation of $Y_{c,interf,k}(n)$ is $x_{c,interf,k}(p)$. Then it is clearly that $x_{c,pre}(p)$

is the time-domain cross-correlation without affected by the frequency offset, $x_{c,interf}(p)$ is the interference caused by the frequency offset and the k-th entry of it is $x_{c,interf,k}(p)$. Set m, m_{pre}, $\mathrm{m}_{interf,k}$ are entries with the largest absolute value in $x_c(p)$, $x_{c,pre}(p)$, $x_{c,interf,k}(p)$, respectively. And the phases of $x_{c,pre}(\mathrm{m}_{pre})$, $x_{c,interf,k}(\mathrm{m}_{interf,k})$ are θ_{pre}, $\theta_{interf,k}$. So the peak position offset caused by the frequency offset can be denoted as the absolute value of $\mathrm{m} - \mathrm{m}_{pre}$.

If $\mathrm{m}_{pre} \neq \mathrm{m}_{interf,k}$, as shown in Fig. 3(a), the k-th entry interference will cause a large change in the peak size and peak position of the cross-correlation result. When $k < 0$, the closer $\theta_{interf,k}$ is to $\theta_{pre} + \pi$, the larger the peak size is, and the larger the peak position changes, the closer $\theta_{interf,k}$ is to θ_{pre}, the smaller the peak size is, and the smaller the peak position changes. When $k > 0$, changes are reversed.

If $\mathrm{m}_{pre} = \mathrm{m}_{interf,k}$, as shown in Fig. 3(b), frequency offset may cause a larger change in the peak size than $\mathrm{m}_{pre} \neq \mathrm{m}_{interf,k}$, but it can't change the peak position of the cross-correlation result. When $k < 0$, the closer $\theta_{interf,k}$ is to $\theta_{pre} + \pi$, the larger the peak size is, the closer $\theta_{interf,k}$ is to θ_{pre}, the smaller the peak size is. When $k > 0$, changes are reversed.

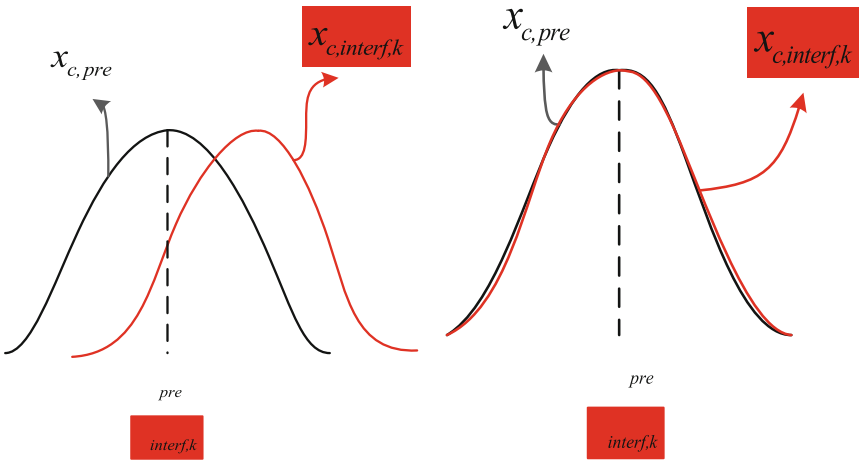

(a) Two peak positions are different (b) Two peak positions are the same

Fig. 3. Peak position relationship between $x_{c,interf,k}(p)$ and $x_{c,pre}(p)$

According to the above analysis, it is known that for a sequence, if $\mathrm{m}_{pre} \neq \mathrm{m}_{interf,k}$, the peak of correlation will be greatly affected by frequency offset, and the larger the peak size is, the larger the peak position changes. If $\mathrm{m}_{pre} = \mathrm{m}_{interf,k}$, it can effectively avoid frequency offset effect on the peak position of correlation.

4 Frequency Offset Effect on the Correlation of ZC Sequences

In this section, the specific effect of frequency offset on the correlation of ZC sequences is analyzed based on the derivation of Sect. 3, and the PRACH preamble detection performance and TA accuracy are roughly predicted. According to the related specifications in 5G NR systems, the 64 preambles used in each time-frequency PRACH occasion can be determined by the root sequence number u and cyclic shift value C_v [1]. Since frequency offset usually is less than half subcarrier spacing, set the type of restricted sets is unrestricted in this paper. Then the 64 PRACH preambles can be obtained as

$$\begin{aligned} x^v(m) &= x_{root}[(m + C_v) \bmod N_{seq}] \\ x_{root}(m) &= e^{-j\frac{\pi um(m+1)}{N_{seq}}} \\ C_v &= vN_{CS} \qquad\quad v = 0, 1, \cdots, 63 \end{aligned} \tag{16}$$

where N_{CS} refers to the length of cycle shift and is determined by the higher-layer parameter [1]. The preamble format used in this paper is PRACH preamble format 0 defined in 5G NR systems. Related parameters are shown in the Table 1.

Table 1. Preamble parameters of the PRACH.

Preamble parameters	Values
N_{seq}	839
f_s	1.25 KHz
u	1
N_{CS}	13

The root sequence can be denoted as

$$\begin{aligned} x_{root}(m) &= \mathrm{e}^{-j\frac{m(m+1)}{839}\pi} \qquad m = 0, 1, \cdots, 838 \\ Y_{root}(n) &= \mathrm{e}^{j\left[1.750298+\frac{n(n+1)}{839}\right]\pi} \qquad n = 0, 1, \cdots, 838 \end{aligned} \tag{17}$$

And the preamble sequences can be denoted as

$$\begin{aligned} x^v(m) &= \mathrm{e}^{-j\left[\frac{13v(13v+1)}{839}+\frac{26vm+m(m+1)}{839}\right]\pi} \\ Y_1^v(n) &= \mathrm{e}^{j\left[1.750298+\frac{26vn+n(n+1)}{839}\right]\pi} \end{aligned} \tag{18}$$

According to (14), $Y_{c,pre}^v(n)$ can be calculated as

$$Y_{c,pre}^v(n) = H\mathrm{e}^{j\frac{26vn}{839}\pi} \tag{19}$$

After IFFT, $x^v_{c,pre}(p)$ is calculated as

$$x^v_{c,pre}(p) = \frac{H}{N}\frac{\sin\left[\left(13v+\frac{839p}{N}\right)\pi\right]}{\sin\left[\left(\frac{13v}{839}+\frac{p}{N}\right)\pi\right]}\mathrm{e}^{j\left(\frac{13v}{839}+\frac{p}{N}\right)838\pi} \quad p=0,1,\cdots,N-1 \tag{20}$$

where the entry with the largest absolute value $x^v_{c,pre}(m^v_{pre})$ satisfies

$$\begin{aligned}
&\left[\left[\frac{13v}{839}+\frac{m^v_{pre}}{N}\right]\right] = 1\\
&m^v_{pre} = N-\left[\left[\frac{13v}{839}N\right]\right]\\
&\left|x^v_{c,pre}(m^v_{pre})\right| = \frac{H}{\mathrm{N}}\left|\frac{\sin\left[\left(13v+\frac{839m^v_{pre}}{N}\right)\pi\right]}{\sin\left[\left(\frac{13v}{839}+\frac{m^v_{pre}}{N}\right)\pi\right]}\right|
\end{aligned} \tag{21}$$

where $[\![]\!]$ denotes the round operator. Considering the interference caused by frequency offset, $Y^v_{c,interf,k}(n)$ is obtained as

$$Y^v_{c,interf,k}(n) = \left\{\begin{array}{ll} H\left|K(k)\right|\mathrm{e}^{j\left(\frac{26vn}{839}+\frac{26vk+2nk+k^2+k}{839}\right)\pi} & \max(0,-k)\le n\le \\ & \min(838,838-k) \\ 0 & \text{else} \end{array}\right\} \tag{22}$$

Then the k-th interference $x^v_{c,interf,k}(p)$ can be denoted as

$$\begin{aligned}
x^v_{c,interf,k}(p) =& \frac{H}{N}\left|K(k)\right|\frac{\sin\left[\left(\frac{13v+k}{839}+\frac{p}{N}\right)(839-|k|)\pi\right]}{\sin\left[\left(\frac{13v+k}{839}+\frac{p}{N}\right)\pi\right]}\\
&\times \mathrm{e}^{j\left[\frac{(13v+k)(838-k)+26vk+k^2+k}{839}+\frac{p(838-k)}{N}\right]\pi}
\end{aligned} \tag{23}$$

where the entry with the largest absolute value $x^v_{c,interf,k}(\mathrm{m}^v_{interf,k})$ satisfies

$$\begin{aligned}
&\left[\left[\frac{13v+k}{839}+\frac{\mathrm{m}^v_{interf,k}}{N}\right]\right] = 1\\
&\mathrm{m}^v_{interf,k} = N-\left[\left[\frac{13v}{839}N\right]\right]-\left[\left[\frac{k}{839}N\right]\right]
\end{aligned} \tag{24}$$

So $\mathrm{m}^v_{interf,k}$ has an offset of $\left[\left[\frac{Nk}{839}\right]\right]$ with respect to m^v_{pre}. According to (23), the bigger k is, the bigger the offset is, and the smaller $|K(k)|$ is. So it is reasonable to consider only two interferences ($x^v_{c,interf,1}$ and $x^v_{c,interf,-1}$) when analyzing frequency offset effect on the peak of ZC sequences correlation, then the final cross-correlation affected by frequency offset can be simplified as

$$x^v_c(p) \approx |K(0)|x^v_{c,pre}(p) + x^v_{c,interf,1}(p) + x^v_{c,interf,-1}(p) + q_{cor}(p) \tag{25}$$

where the peak of final cross-correlation affected by frequency offset is related to the random access preamble number. According to the above calculations and

general conclusion in Sect. 3, frequency offset has an impact on both the peak position and peak size of ZC sequences correlation results. Besides, the PRACH preamble miss detection rate and timing error of UEs with different random access preamble numbers are differently affected by the same frequency offset. The better the detection performance, the lower the TA accuracy.

5 Simulation Results and Analysis

In this section, simulations are performed to verify the rationality of the above analysis about frequency offset effect on the PRACH, including the PRACH preamble sequence detection performance and TA error. Simulation parameters are shown in the Table 2.

Table 2. Simulation parameters of the PRACH.

Simulation parameters	Values
The PRACH preamble format	Format 0
Antenna configuration	1Tx*2Rx
Carrier frequency	4 GHz
Bandwidth	40 MHz
Frequency offset	500 Hz
Channel model	AWGN
Sampling interval (dt)	0.0163 μs

In this part, the PRACH preamble detection BLER and CDF of TA error are taken as two performance metrics. The detection threshold is set according to the request that the false alarm probability shall be less than or equal to 0.001 [9], and the preamble detection BLER is counted by comparing the PAR of correlation with the detection threshold. TA error is denoted by the absolute value of $\mathrm{m} - \mathrm{m}_{pre}$. The peak size and peak position of the correlation result at the receiving end between the derived result in this paper and the simulation result are compared. Besides, the relationship between detection BLER and TA error is analyzed. Simulations are shown below. Where simulation represents the simulation result calculated by MATLAB according to Fig. 2, derivation denotes the derived result in this paper.

Firstly, peak sizes corresponding to different random access preamble numbers are shown as Fig. 4(a). As can be seen from Fig. 4(a), peak sizes of the simulation results and the derived results show the same trend with the change of v, and they are almost the same in a large range of v from 5 to 60. Besides, peak sizes of different preamble numbers are differently affected by the same frequency offset, which proves the rationality of the above calculations and analysis. Then, the preamble detection BLER is presented in Fig. 4(b), when $v = 0$,

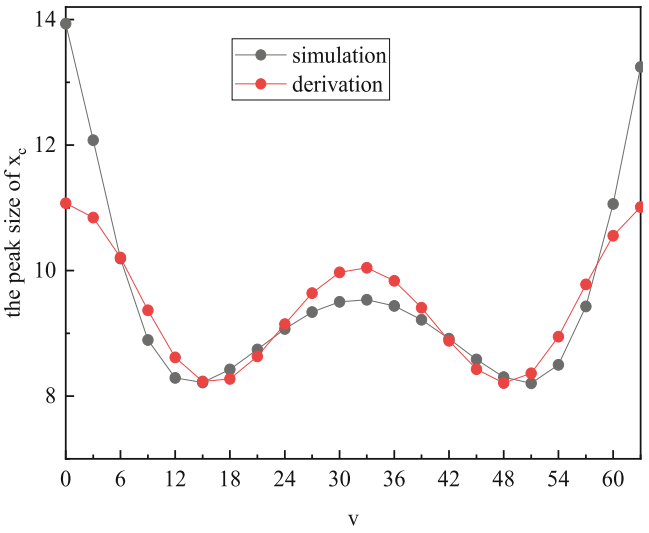

(a) Peak size at 500 Hz frequency offset

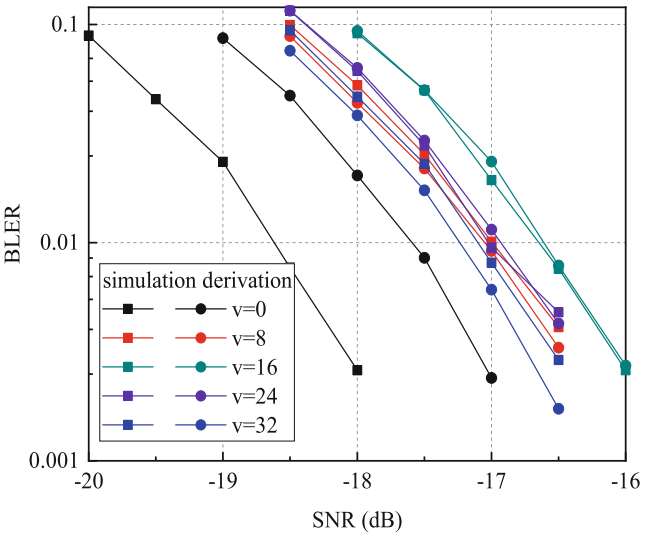

(b) Preamble detection BLER

Fig. 4. PRACH preamble detection performance

there is a significant difference in the detection BLER between the simulation results and the derived results. When v takes other values, there is basically no difference, which is consistent with the feature of peak size in Fig. 4(a).

Fig. 5(a) shows the TA error affected by 500 Hz frequency offset without considering the noise. It shows that the derived results are very close to the

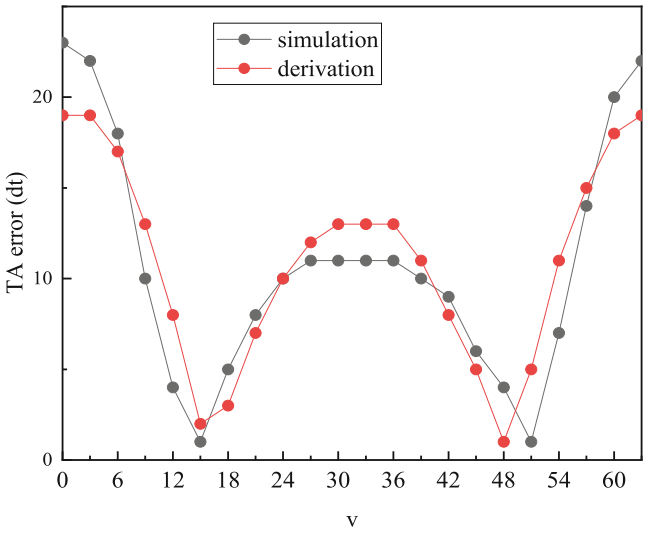

(a) TA error at 500Hz frequency offset

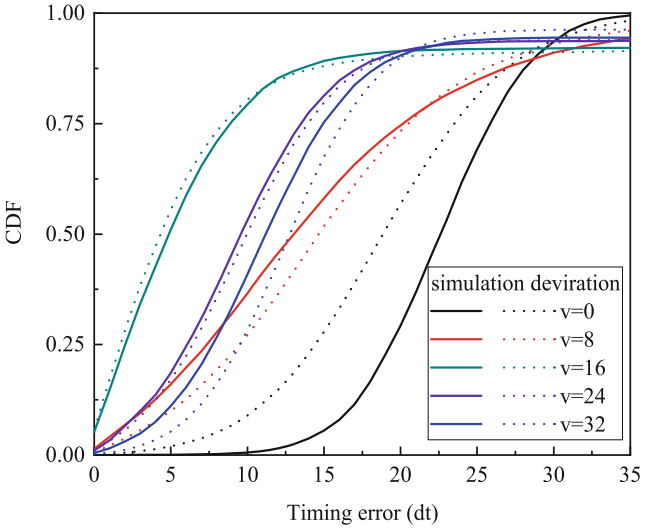

(b) TA error CDF at 18 dB SNR

Fig. 5. TA error

simulation results, and TA errors of different preambles are differently affected by the same frequency offset. Then, the TA error CDF at 18 dB SNR is presented in Fig. 5(b), which shows that the derived result is very close to the simulation results in most cases. Comparing Figs. 4(b) and 5(b), it can be found that under the frequency offset effect, for different preamble sequences, the lower the

detection BLER, the larger the TA error, which proves the correctness of analysis in Sects. 3 and 4.

6 Conclusion

In this paper, the impact of frequency offset on PRACH in 5G NR systems is analyzed. Considering that preamble detection BLER and TA error are closely related to the peak of correlation result, this paper aims to analyze frequency offset effect on the peak of PRACH preamble correlation. Through derivation and calculation, the following analytical results are obtained. Inter-carrier interference coefficients of multiple interference entries caused by the frequency offset have almost the same phase. Correlation results of different sequences are differently affected by frequency offset, if frequency offset affects the peak position of correlation, the larger the peak size is, the larger the peak position changes. The preamble detection BLER and TA error of UEs with different random access preamble numbers are differently affected by the same frequency offset, the lower the detection BLER, the higher TA error. The simulation results show the rationality of analysis in this paper. The analytical method used in this paper plays a certain role in analyzing frequency offset effect on correlation. Moreover, the analytical results about the frequency offset effect on PRACH are helpful for studying how to effectively resist frequency offset. But there is room for improvement.

References

1. 3GPP TS 38.211, 3rd Generation Partnership Project, Technical Specification Group Radio Access Network, NR, Physical channels and modulation, Release 15 (2019)
2. 3GPP TS 38.213, 3rd Generation Partnership Project, Technical Specification Group Radio Access Network, NR, Physical layer procedures for control, Release 15 (2019)
3. Thota, J., Aijaz, A.: On performance evaluation of random access enhancements for 5G URLLC. In: IEEE Wireless Communications and Networking Conference (WCNC), Marrakech, Morocco, pp. 1–7 (2019)
4. Tao, J., Yang, L.: Improved Zadoff-Chu sequence detection in the presence of unknown multipath and carrier frequency offset. IEEE Commun. Lett. **22**(5), 922–925 (2018)
5. Tang, Q., Long, H., Yang, H., Li, Y.: An enhanced LMMSE channel estimation under high speed railway scenarios. In: 2017 IEEE International Conference on Communications Workshops, Paris, France, pp. 999–1004 (2017)
6. Cao, A., Xiao, P., Tafazolli, R.: Frequency offset estimation based on PRACH preambles in LTE. In: 2014 11th International Symposium on Wireless Communications Systems, Barcelona, Spain, pp. 22–26 (2014)
7. Hua, M., Wang, M., Yang, W., You, X., Shu, F., Wang, J., et al.: Analysis of the frequency offset effect on random access signals. IEEE Trans. Commun. **61**(11), 4728–4740 (2013)

8. Zhang, Y., Zhang, Z., Hu, X.: An improved preamble detection method for LTE-A PRACH based on Doppler frequency offset correction. In: Liu, X., Cheng, D., Jinfeng, L. (eds.) ChinaCom 2018. LNICST, vol. 262, pp. 573–582. Springer, Cham (2019). https://doi.org/10.1007/978-3-030-06161-6_56
9. 3GPP TS 38.104, 3rd Generation Partnership Project, Technical Specification Group Radio Access Network, NR, Base Station radio transmission and reception, Release 15 (2019)